Journal of Physics: Conference Series **655** (2015) 012022 doi:10.1088/1742-6596/655/1/012022

Design and experimental analysis of a screened heat pipe for solar applications

D Jafari, S Filippeschi, A Franco, P Di Marco

Università di Pisa, DESTEC, Largo Lucio Lazzarino 2, 56122 Pisa, Italy

E-mail: d.jafari@studenti.unipi.it

Abstract. This paper summarizes the design, the construction and the preliminary results of a transient and steady state investigation of the heat transfer mechanisms of a horizontal heat pipe (HP). The experiments are performed using a custom-made HP constituted by copper tube with outer diameter and length as 35 mm and 510 mm, respectively, with the inner surface covered by three layers stainless steel mesh wick (100 mesh/inch). Water is used as a working fluid. The evaporator section is heated by electrical resistances wrapped around the tube and the cooling system consists of an insulated water manifold with inner diameter of 39 mm, connected to chilled water bath to maintain the inlet temperature of the circulating cooling water at 25 ˚C for various heat loads (30-100 W). The aims of this activity is to obtain data to verify the steady state HP analytical model already presented by authors at a fixed filling volume and to determine the effect of the heat transfer load on the heat transfer performance of screen mesh HPs. The heat transfer coefficients are determined using thermocouples on the outer wall and within the core of the HP. The agreement between the analytical results and the preliminary experimental data appears to be very good.

1. Introduction

Phase change heat transfer is suitable for transferring large amount of heat because of the high heat transfer coefficients associated with the evaporation and condensation processes. Heat pipe (HP) is one of such a passive device, which utilize phase change of the working fluid inside of a sealed container (generally a pipe), efficiently transporting large amount of heat from evaporator section to the condenser section; The condensed liquid is drawn back to the evaporator by the capillary force in the wick structure laid at the internal periphery of the device [1-3].

HPs have been widely applied for several engineering application such as electronics cooling, air conditioning and power generation [4-7]. HPs can be also used for thermal control, in particular in connection with solar energy systems like solar collectors [8-11], solar walls [12, 13] or photovoltaic systems [14, 15].

The wide use of HPs has led to increased demand to study its thermal performance in order to efficiently designing them, mainly in connection with solar application for medium temperature (50-150˚C). Many theoretical studies of the operation of low temperature and high temperature HPs have been reported such as simple lumped model [16] and analytical model [17-19]. However, the focus of the present study is on experimental investigations of the transient and steady state operation of HPs,

with emphasis on obtaining data to verify an existing steady state HP model presented by the authors in [20].

The thermal behaviour in a HP is determined by many parameters, such as heat input, filling ratio of the working fluid, geometry, orientation, characteristics of the capillary structure, and the thermophysical properties of the working fluid. The heat transfer characteristics of the HP have been experimentally investigated by several researchers. Among the others, El-Genk and Huang [21] focused the attention on the transient response of a HP (screen mesh) at different input powers and cooling rates. Wang and Vafai [22] experimentally investigated the transient thermal performances of flat plate HPs. They introduced the concept of HP time constants to describe its transient behaviour and to understanding the start-up and shut-down phenomena of HPs. Kempers et al. [23] considered the effect of the number of mesh layers and filling ratio on the heat transfer performance of copper HPs (screen mesh wicks) using water as working fluid. It was found that the effective thermal resistance decreases with an increase in heat flux, and the thermal resistance is larger for fewer mesh layers. Further, Kempers et al. [24] analysed the heat transfer mechanisms in the condenser and evaporator sections of a 3 layers of screen-mesh HP. Wong and Kao [25] investigated HPs consisting of a two-layer copper mesh wick of 100 and 200 mesh/inch screens using ether as working fluid. They discussed the effects of different wicks and fluid filling ratios on the evaporation/boiling characteristics.

For the design of HPs for particular applications several theoretical models have been developed based on the solution of conservation equations in two phase systems, but they must be joined with an experimental characterization of the heat and mass transfer mechanisms. In fact, the link between fluid-dynamics, thermal behaviour and gravitational effects are not completely known and obtained data are difficult to be used for general cases or extended to particular cases like medium temperature applications. For this reason the authors first developed a model for sensitivity analysis of HP [20] and then designed and constructed an experimental facility to validate the model. This paper describes and summarizes the progress and the preliminary results of an investigation into the heat transfer process of a screen mesh HP for solar thermal application. The test rig allows measurements of the wall temperature and the vapour temperature in the different regions of the HP (evaporator, adiabatic, and condenser sections) as well as vapour pressure and also the thermal power removed by means of the cooling manifold. The purpose of the present study is to characterize the effect of heat load on the transient and steady state operation of copper HPs. The evaporation heat transfer coefficient of the HP is evaluated and the working characteristics and its heat transfer performance are discussed.

2. Principles and operation of HP for the specific application

Figure 1 shows the operation of a cylindrical HP. The components of a HP are pipe wall and end caps, a wick structure and a small amount of working fluid. The length of a HP could be divided into three parts: the evaporator, adiabatic and condenser sections. Heat applied to the evaporator section is conducted through the pipe wall and wick structure, where the working fluid evaporates. The resulting vapour pressure drives the vapour to the condenser, where it releases its latent heat of vaporization to the provided heat sink [2]. The capillary pressure created by the wick pumps the condensed fluid back to the evaporator section. This process will continue as long as there is a sufficient capillary pressure to drive the condensate back to the evaporator. The selection of the wick structure could be an important parameter which depends on several factors: working fluid, pipe material and working conditions.

For designing a HP for specific application like solar collectors, one of the important elements is the characterisation of the wick structure, in particular its permeability, the developed capillary pressure and the effective conductivity [3]. In order to have a large capillary pressure difference, capillary radius must be small. Permeability must be large in order to have a lower liquid pressure drop, a better distribution of the liquid and therefore, higher heat transport capability. A large value of effective thermal conductivity gives a small temperature drop across the wick, which is a favourable condition for the HP performance.

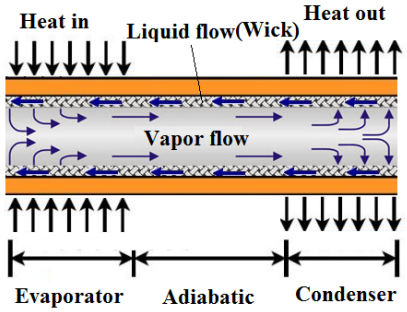

Figure 1. Cylindrical HP**:** a schematic view.

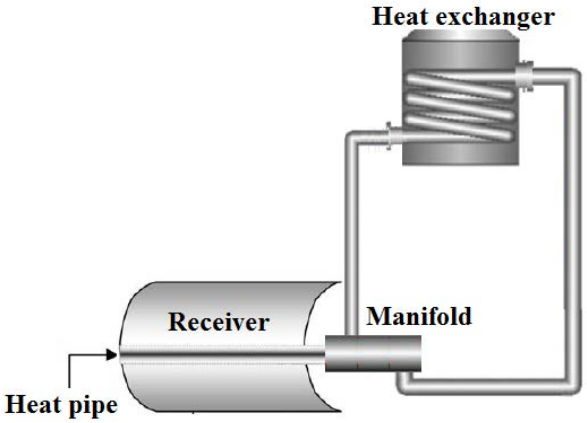

Figure 2. Schematic view of concentrating systems.

Table 1. Expressions for HP wick design (screen mesh)

Parameter	Expression
Effective thermal conductivity	$k_{eff} = k_l\left[(k_l + k_w) - (1-\varepsilon)(k_l - k_w)\right]/(k_l + k_w) + (1-\varepsilon)(k_l - k_w)$
Effective capillary radius	R_{eff}=1/2N
Permeability	$K = d_w^2\varepsilon^3/122(1-\varepsilon)^2$
Porosity	$\varepsilon = 1 - S\pi Nd_w/4$

The wick thickness also plays an important role in the determination of the thermal resistance and heat transfer capacity. The screen mesh detailed parameters are calculated according to references [1-3] as evidenced in table 1. Wang and Peterson [26] found that increasing the thickness of the porous layer would correspondingly increase the maximum heat flux based on a capillary limit. Kempers et al. [23] showed that there is a small increase in thermal resistance when increasing the number of mesh screens; however, the maximum heat transfer also increases. The idea pursued in this paper is to conduct an analysis on the operating HP in order to be able to identify criteria for the analysis of thermal performances of such systems in configurations typical of concentrating solar collectors (ranged from 200-10000 W/m^2). The concentrating solar systems using HP are composed a concentrator and a receiver and the receiver is the key component to transfer the energy collected by the concentrator to the heat storage systems. Two particular aspects, that can also be joined together, could be considered for concentrating collectors: the concentration of solar radiation and the use of a fluid with phase change as energy vector. The use of a two-phase fluid flow allows high thermal fluxes to be transferred with very low change in the average temperature, allowing a higher concentration ratio. Figure 2 shows the proposed system including a reflector and a HP.

3. Experimental apparatus

Basing on the objective of the present study and previous discussion and considering the results of the main experimental activities available in the literature the authors have designed, a specific experimental setup aimed to analyse the thermal behaviour of HP. The pipe wall is made of copper with an outer diameter of 35 mm, a thickness of 1 mm and a length of 510 mm. The lengths of evaporator and condenser section are 300 mm and 160 mm, respectively. The working fluid is distilled water. Three layers of stainless steel wick with 100 mesh/inch size is prepared, formed and rolled onto a rod, inserted through the pipe and by means of a specially built device, in order to ensure that the wick and the wall are in good thermal contact. Table 2 and table 3 list the detailed HP and wick parameters. After having assembled, cleaned and sealed the HP using brazing techniques, the pipe is initially evacuated. This process is started at ambient temperature, and then the pumping is continued

to 10^{-4} mbar while the pipe is heated, to favor outgassing. The HP is then filled with the desired amount of degassed, ultra-pure water. Figure 3 shows a schematic diagram of the experimental setup.
The rig consisted of the HP, electrical heating with a voltage controller, cooling flow circuit, vacuum device and measuring system. The evaporator section is uniformly heated using four silicon type thermofoil heaters (model MINCO HK5488R17.2L12A) clamped to the HP using Teflon type insulation. The power input is supplied by a DC Power supply (Agilent DC6575A) which has an accuracy of ±1 percent of reading. In the condenser section, heat is convectively removed by water extracted from a cooling bath (HAKKE F-3C DIN 58966), by means of a 160 mm long copper manifold mounted around the HP, with outside diameter and wall thickness of 42 and 1.25 mm. During the thermal performance tests the temperature of the cooling bath is maintained at an imposed value and the mass flow rate can be exactly controlled. An electromagnetic flow meter (Siemens SITRANS F M MAGFLO5000) allows measurement the mass flow rate of the cooling water with an accuracy of about 1%. The thermocouples in the manifold inlet and outlet and mass flow measurement allow to calculate the power output from condenser section and to compare it with the input electrical power.
All the HP vapours and wall temperatures are measured with T-type thermocouples, which have been calibrated with an accuracy of ±0.2˚C. The external surface temperatures of the HP are measured with eight wire thermocouples (T_{w1} to T_{w8}) mounted along the wall in the evaporator, adiabatic and condenser sections. The vapour temperatures are measured by additional five T-type stainless steel thermocouples (T_{v1} to T_{v5}) mounted axially within the HP vapour space. This handmade multipoint thermocouple are attached to the outer surface a PEEK probe (outer diameter of 3 mm) which exists in the condenser end cap and is swaged to provide a well leak seal. The location of wall and vapour thermocouples is shown in figure 5. In the evaporator end cap a pressure transmitter (PTX7511 accuracy of ±0.15%) is installed to measure vapour pressure. All the signals to monitor HP temperature and pressure and cooling mass flow rate are acquired by the Agilent HP32790 data acquisition system, and stored in a computer.

3.1. Experimental procedure

The experimental procedure began after charging the working fluid in the HP. Following evacuation, 42 cm^3 (filling ratio of 10%) of degassed and distilled water are inserted into the pipe through a special valve arrangement, to avoid air contamination. The amount of water is enough in order to ensure that the wick completely saturated. Figure 4 shows the rig used for HP evacuation and charging in the present study. The cooling water supplied to the water jacket has a constant flow rate of 0.02 kg/s and a temperature of 24.8 ˚C. At the beginning of the test, cooling water is pumped in the condenser jacket before power is supplied. The transient is initiated by increasing the electric power in the evaporator section from 30 to 100 W. The experiment continues until steady state is reached and then a further heat power is applied. The system is considered to have attained steady state when each thermocouple temperature fluctuation is no more than 0.5 ˚C within 5 min. At the steady state and transient operation, the power input, the water flow rate in the cooling jacket, and the temperature at the various locations are recorded. Energy balance between the heat input by electrical heaters and the heat removed by sink is monitored to ensure an energy balance of at least 90 percent.

3.2. Data reduction and uncertainty analysis

The measured variables in the experimental analysis are: heat rate applied to the evaporator section (Q_{in}), heat output of the condenser section (Q_{out}), inlet of coolant water temperature (T_{in}), outlet temperature (T_{out}), mass flow rate of the coolant water ($\dot{m}$), wall surface temperatures (T_w), vapour temperature (T_v) and vapour pressure. The heat transfer capacity of evaporator section for a HP is determined by heat transfer coefficient (h_e). From the measured data of wall temperature and vapour temperature (equivalent to the wall temperature of adiabatic section), the heat transfer coefficient in the evaporator can be evaluated using the following equation:

$$h_e = Q_{av} / \pi d_i L_e (T_{w,e} - T_v) \quad (1)$$

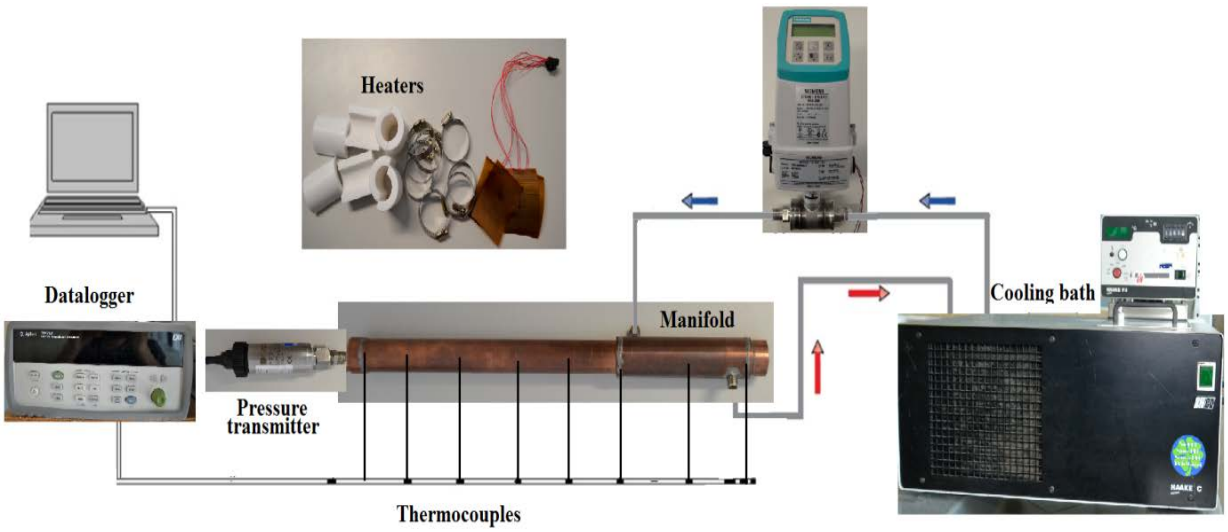

Figure 3. Overall experimental setup.

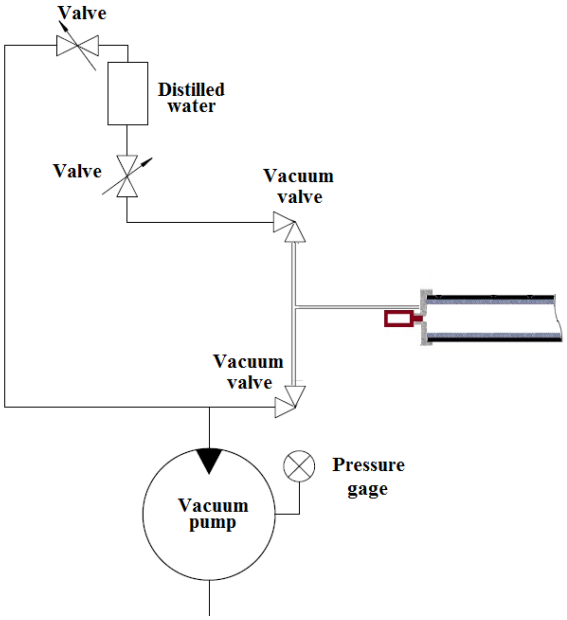

Figure 4. HP filling facilities.

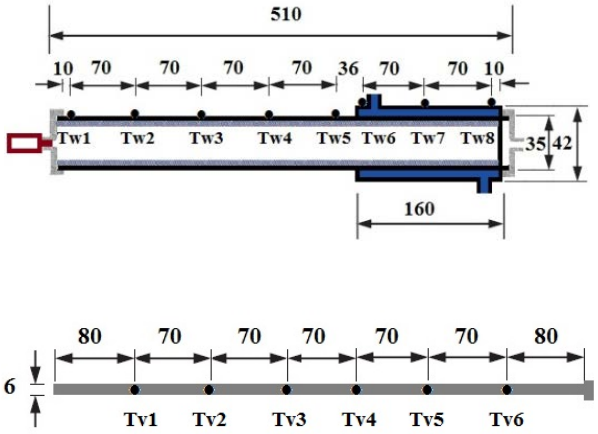

Figure 5. Thermocouple positions along the HP

Table 2. Design summery of HP

Pipe material	Copper
Working fluid	Water
Fluid charge (cm^3)	42
Total length (mm)	510
Evap. length (mm)	225
Cond. length (mm)	160
Outside diameter (mm)	35
Inside diameter (mm)	33

Table 3. Design summery of screen mesh wick

Wick material	Stainless steal
Mesh number (mesh/inch)	100
Effective capillary radius (mm)	0.127
Screen wire diameter (mm)	0.11
Screen wick thickness (mm)	0.66
Porosity	0.63
Permeability	2.01×10^{-10}
Effective thermal conductivity	1.38

where $T_{w,e}$ is average evaporator wall temperature defined considering four temperature as described in figure 5 (T_{w1}, T_{w2}, T_{w3} and T_{w4}), T_v is average vapour temperature (T_{v1}, T_{v2} and T_{v3}) and Q_{av} is average heat transfer rate

$$Q_{av} = Q_1 + Q_2/2 \tag{2}$$

The rate of heat transfer to the evaporator section is obtained from the following relation:

$$Q_1 = VI \tag{3}$$

where V is voltage and I is current. The rate of heat removal from the condenser section is calculated from the following relation:

$$Q_2 = \dot{m}C_p(T_{out} - T_{in}) \tag{4}$$

The experimental uncertainties of the various parameters: heat input, thermal resistance and heat transfer coefficients are calculated. The relative experimental uncertainty can be described for the variable $R = R(x_1, x_2, \ldots, x_n)$ as:

$$U_R/R = \sqrt{\sum_{i=1}^{n}\left[(x_i/R)(\partial R/\partial x_i)\right]^2(P_i/x_i)} \tag{5}$$

where P is the bias limit of the variable R. From above equations and mentioned uncertainty of apparatus, the relative uncertainties of the output heat flux from condenser section and evaporation heat transfer coefficient are estimated 4.8% and 5.5%, respectively for the temperature and heat load ranged 25-40˚C and 30-100W, respectively.

4. Experimental results and analysis

The objective of the experiments is to characterize the heat loading on the transient and steady state operation of a screen mesh HP. Further, to obtain data to verify an existing steady state HP model previously presented by authors [20].

4.1. Transient behaviour of HP

Before test, the entire HP is set at ambient temperature, and the interface between the liquid in the wick and the vapour is at saturation. Figure 6 shows the results of the transient response of the HP to a step function increase in electric power input up to 100 W. The HP reached steady-state approximately 600 s after the initiation of the transient, for an input heat load of 30 W. At steady state, the output heat flux is only about 2.1 W lower than the electric power input (see table 3). Figure 7 shows the measured axial distributions of the wall and vapour temperatures at different times during the transient reported in figure 6. As can be seen in figure 7a, the measured wall temperatures in the evaporator and condenser sections are almost uniform. The vapour temperatures are nearly uniform along the entire length of the HP, except for the condenser section (figure 7b): variations are less than 1K. The reason for this low vapour temperature in the condenser section for lower heat loads will be discussed in section 4.2.

4.2. Steady state temperature distribution along the outside wall surface

Experimental results of the temperature distribution along the wall surface of HP at horizontal orientation are compared in figure 8a. The tests are conducted at different heat inputs and constant cooling water temperature (24.8˚C). The results indicate that, as expected, the evaporator wall temperature rises with the increase of heat flux, and the temperature distribution of the HP is nearly uniform and decreases slightly towards the adiabatic section. The temperature reaches the minimum value at the condenser section. The wall temperature of the condenser is approximately uniform for all heat transfer rates, with an average value of 25 ˚C. It should be noted that the condenser temperature is the temperature of outer manifold wall. The axial vapour temperature distribution corresponding to figure 8a is shown in figure 8b. The vapour core temperatures in the evaporator section are nearly equal and increase with the heat input as expected. The core temperatures in the condenser section at the lowest heat inputs of 30 and 40 W are significantly lower than that in the evaporator section. This low vapour temperature in the condenser section could be due to the presence of residual non-condensable gases which tend to accumulate at the condenser end of the heat pipe. At low heat fluxes,

the non-condensable gases occupy a larger part of the condenser due to the lower vapour pressure. As the heat flux increases (for heat input above 40W), the vapour core temperatures in the condenser section increase. The incondensable gases seem to have a minor role on these conditions and the active region of the condenser is increased. The vapour temperatures are also nearly uniform and closer to the adiabatic wall temperature (T_{w5}).

4.3. Evaluation of evaporation heat transfer coefficient

The thermal resistance of the evaporator section can be expressed in terms of a heat transfer coefficient. The measurements of heat flux and of average wall and vapour temperature, temperature in the evaporator and are used to calculate the heat transfer coefficients in the evaporator section of the HP by using Eq. (1). The heat transfer coefficients for the HP are plotted versus average temperature of evaporator section as shown in figure 9. As can be seen, the evaporation heat transfer coefficient is non-linear and increases as the temperature (heat flux) increases. At higher heat fluxes (1850 W/m^2 to 2100 W/m^2), the heat transfer increases rapidly, indicating the thermal resistance of the HP is decreasing.

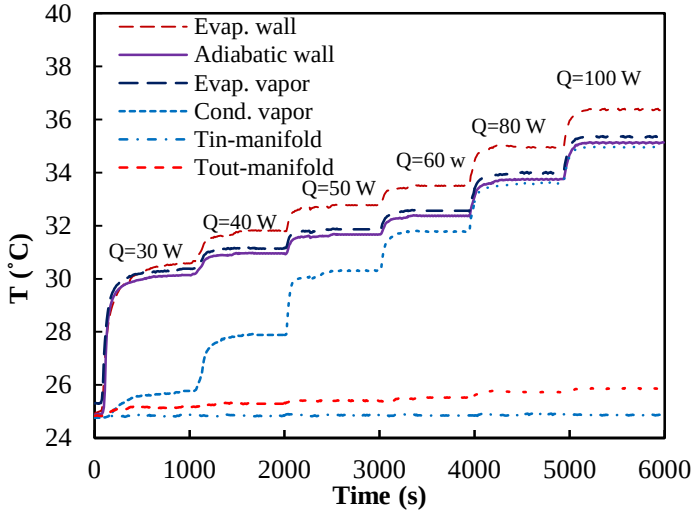

Figure 6. Transient temperature behaviour of HP for different heat input (T_c = 24.8 °C).

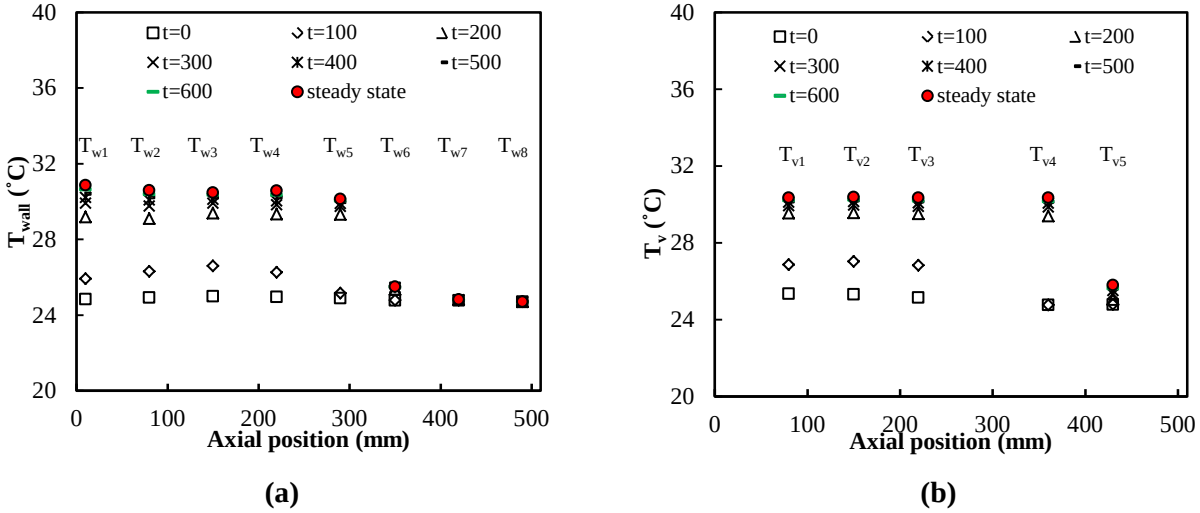

(a) **(b)**

Figure 7. Transient axial distributions of wall temperatures (a) and vapour temperatures (b), Q=30 W.

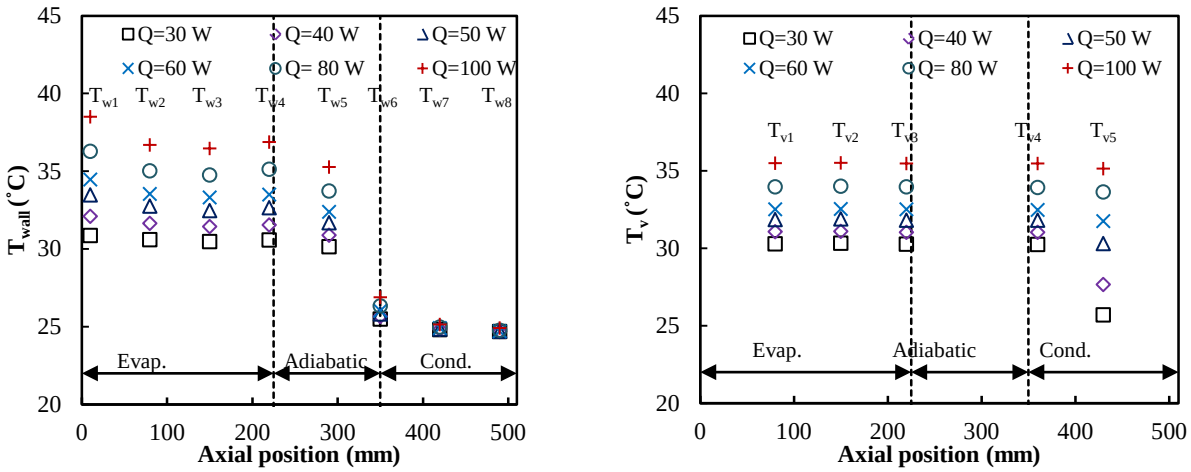

Figure 8. Steady state axial distribution of wall temperatures (a) and (b) vapour temperatures (b) different heat input.

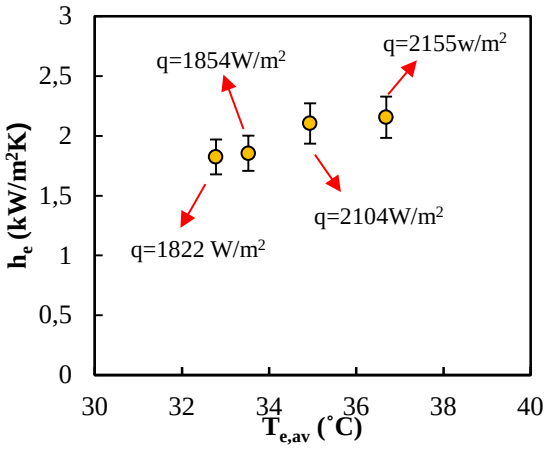

Figure 9. The heat transfer coefficients against average temperature of evaporator section

5. Comparisons between the experimental data and the expected analytical results

As already mentioned in previous section, a steady–state analytical model has been developed and presented in [20] to predict the performance of HPs. The model couples two–dimensional heat conduction in the HP wall with the liquid flow in the wick and the vapour hydrodynamics. The experimental data obtained in the present analysis have been compared with the results expected with the model for different heat input. In theoretical analyses, it is assumed that the condenser is cooled by water, according to the experimental apparatus. Thus, a convection heat transfer coefficient is defined as boundary condition on the condenser wall. The condenser heat transfer coefficients (h_{inf}) are determined based on the experimental data (output heat flux in the condenser section Q_{out}, and average cooling water temperature $T_{c,av}$) are shown in table 4.

Figure 10a and figure 10b show the comparison between the HP wall and vapour temperatures obtained from analytical model with the experimental data, respectively. The agreement of the results with experimental data is very good. A difference less than about 1K is observed between the evaporator vapour and wall temperatures predicted by theoretical models and experimental data, which can be acceptable at this step of analysis considering the experimental error and approximations in the analytical model. It should be noted that the condenser temperature is not reported in the current experimental study because the temperature of condenser section is obtained based on wall manifold temperature which is different from HP condenser section.

Table 4. Condenser heat transfer coefficients for different heat inputs.

Evaporator	Condenser			
Q_{in} (W)	Q_{out} (W)	T_{in}	$T_{c,av}$ (˚C)	h_{inf}(W/m^{2}K)
60	56.5	24.8	25.18	476.9
80	74.59	24.8	25.3	531.33
100	92.81	24.8	25.41	571.88

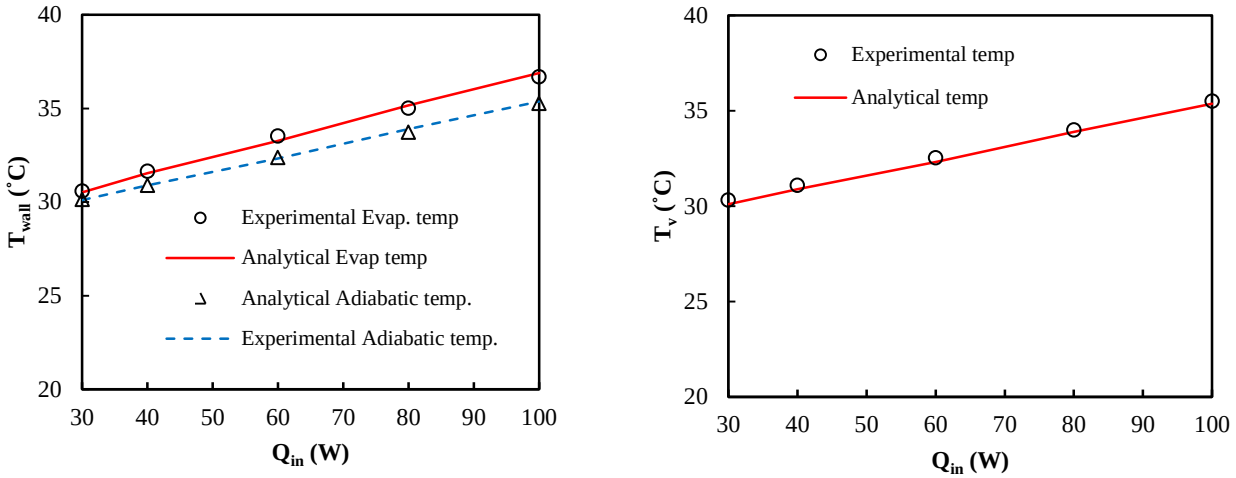

(a) (b)

Figure 10. Variation of wall temperature (a) and vapour temperature (b) with heat input obtained from the analytical and experimental studies for the evaporator and adiabatic section.

6. Conclusions

The study proposed in this paper presents a detailed experimental apparatus and preliminary experimental results about the heat transfer performances of a HP designed for a particular solar application. The experimental apparatus has been developed to investigate the thermal performance of a cylindrical copper HP using water as a working fluid. Transient experiments were performed using a uniformly heated evaporator section and a convectively cooled condenser section (temperature of 24.8˚C). The effect of the heat load (30-100 W) on the heat transfer performance of HPs was experimentally investigated by testing a HP with 3 layers of wire screen mesh (100 mesh/inch). The axial distribution of the wall and vapour temperatures were measured and discussed in detail. By experimenting on different heat loads under steady-state and transient conditions, it was observed that the temperature variation along the wall surface of the evaporator section of the HP was nearly uniform and decreased slightly along the adiabatic section. In the experiment, the vapour temperature was uniform along the HP, except at low heat loads (30 and 40 W) where it was significantly lower than that in the evaporator section, presumably due to the presence of residual non-condensable gases. The results obtained are in very good agreement with data obtained by a numerical HP model previously presented by the authors. After these preliminary results, the authors will further develop the experimental analysis to evaluate the maximum heat transfer capacity of HP for different filling ratios (10-50%), inclination angles (0-90˚) and low-to-medium cooling water temperatures (25-90˚C).

7. References

[1] Peterson GP 1994 *Heat Pipes: Modelling, Testing and Applications* (USA: John Willey & Sons)
[2] Faghri A 1995 *Heat Pipe Science and Technology* (Washington, DC: Taylor and Francis)

[3] Reay DA and Kew PA 2006 *Heat Pipes, Theory Design and Applications* (New York: Elsevier)
[4] Vasiliev LL 2005 *Heat Pipes in Modern Heat Exchangers* Appl. Therm. Eng. **25**(1) 1-19.
[5] Wan JW, Zhang JL and Zhang WM 2007 *The effect of heat-pipe air-handling coil on energy consumption in central air-conditioning system* Energy Build. **39** 1035–40.
[6] Mochizuki M, Nguyen T, Mashiko K, Saito Y, Nguyen T and Wuttijumnong V 2011 *A Review of Heat Pipe Applications Including New Opportunities* Frontiers in Heat Pipes **2** 013001.
[7] Remeli MF, Tan L, Date A, Singh B and Akbarzadeh A 2015 *Simultaneous power generation and heat recovery using a heat pipe assisted thermoelectric generator system.* Energy Convers. Manage. **91** 110–19.
[8] Riffat S, Zhao X and Doherty PS 2005 *Developing a theoretical model to investigate thermal performance of a thin membrane heat-pipe solar collector* Appl. Therm. Eng. **25** 899–915.
[9] Azad E 2008 *Theoretical and experimental investigation of heat pipe solar collector* Exp. Thermal Fluid Sci. **32** 1666-72
[10] Arab M and Abbas A 2013 *Model-based design and analysis of heat pipe working fluid for optimal performance in a concentric evacuated tube solar water heater* Solar Energy **94** 162–76.
[11] Brahim T, Dhaou MH and Jemni A 2014 *Theoretical and experimental investigation of plate screen mesh heat pipe solar collector.* Energy Convers. Manage. **87** 428–38.
[12] Wang Z, Duan Z, Zhao X and Chen M 2012 *Dynamic performance of a facade-based solar loop heat pipe water heating system* Solar Energy **86** 1632–47.
[13] He W, Hong X, Zhao X, Zhang X, Shen J and Ji J 2015 *Operational performance of a novel heat pump assisted solar façade loop-heat-pipe water heating system.* Appl. Energy **146** 371–82.
[14] Akbarzadeh A and Wadowski T 1995 *Heat pipe-based cooling systems for photovoltaic cells under concentrated solar radiation* Appl. Therm. Eng. **16**(1) 81–7.
[15] Gang P, Huide F, Tao Z and Jie J 2011 *A numerical and experimental study on a heat pipe PV/T system* Solar Energy **85** 911–21.
[16] Zuo ZJ and Faghri A 1998 *A network thermodynamic analysis of the heat pipe* Int. J. Heat Mass Trans. **41**(11) 1473-84.
[17] Huang XY and Liu CY 1996 *The pressure and velocity fields in the wick structure of a localized heated flat plate heat pipe* Int. J. heat mass trans. **39** 1325–30.
[18] Zhu N and Vafai K 1999 *Analysis of cylindrical heat pipes incorporating the effects of liquid – vapor coupling and non-Darcian transpor –a closed form solution* Int. J. heat mass trans. **42** 3405–18.
[19] Shabgard H and Faghri A 2011 *Performance characteristics of cylindrical heat pipes with multiple heat sources* Appl. Therm. Eng. **31** 3410–18
[20] Di Marco P, Filippeschi S, Franco A and Jafari D 2014 *Theoretical Analysis of Screened Heat Pipes for Medium and High Temperature Solar Applications* J Phys Conf Ser **547** 012010.
[21] El Genk MS and Huang L 1993 *An experimental investigation of the transient response of a water heat pipe* In. J. Heat Mass Trans. **36**(15) 3823-30.
[22] Wang Y and Vafai K 2000 *An experimental investigation of the thermal performance of an asymmetrical flat plate heat pipe* Int. J. Heat Mass Trans. **43** 2657-68.
[23] Kempers R, Ewing D and Ching CY 2006 *Effect of number of mesh layers and fluid loading on the performance of screen mesh wicked heat pipes* Appl. Therm. Eng. **26** 589–95.
[24] Kempers R, Robinson AJ, Ewing D and Ching CY 2008 *Characterization of evaporator and condenser thermal resistances of a screen mesh wicked heat pipe* Int. J. Heat Mass Trans. **51**6039–46.
[25] Wong SC and Kao YH 2008 *Visualization and performance measurement of operating mesh-wicked heat pipes.* Int. J. Heat Mass Trans. **51** 4249–59.
[26] Wang YX and Peterson GP 2003 *Analytical model for capillary evaporation limitation in thin porous layers* J. Thermophys. Heat Transfer **17**(2) 145–9.